Liquid Crystals
Publication details, including instructions for authors and subscription information:
http://www.informaworld.com/smpp/title~content=t713926090

Metastable phases in kinetics of phase transformations in the frozen liquid crystal 4-ethoxybenzylidene-4'-*n*-butylaniline

A. Elouatib[a]; C. Gors[a]; R. Fouret[a]
[a] Laboratoire de Dynamique et Structure des Matériaux Moléculaires, Université de Lille Flandres Artois, Villeneuve d'Ascq Cedex, France

To cite this Article Elouatib, A. , Gors, C. and Fouret, R.(1991) 'Metastable phases in kinetics of phase transformations in the frozen liquid crystal 4-ethoxybenzylidene-4'-*n*-butylaniline', Liquid Crystals, 9: 4, 539 — 550
To link to this Article: DOI: 10.1080/02678299108033151
URL: http://dx.doi.org/10.1080/02678299108033151

LIQUID CRYSTALS, 1991, VOL. 9, NO. 4, 539–550

Metastable phases in kinetics of phase transformations in the frozen liquid crystal 4-ethoxybenzylidene-4′-*n*-butylaniline

by A. ELOUATIB, C. GORS and R. FOURET*
Laboratoire de Dynamique et Structure des Matériaux Moléculaires,
Université de Lille Flandres Artois, 59655 Villeneuve d'Ascq Cedex, France

(*Received 13 July 1990; accepted 22 November 1990*)

The nematogen 4-ethoxybenzylidene-4′-*n*-butylaniline gives by fast cooling a frozen phase called C_1 different from a glassy nematic state. The X-ray diffraction spectra of a non-aligned sample and a sample aligned by a magnetic field show that the C_1 phase is a monolayer smectic phase: molecules are inclined to the normal of the smectic planes by an angle of $35° \pm 5°$. On reheating we obtain metastable phases more and more ordered; those phases C_2 and C_3 are crystalline. The kinetics for the metastable phases correspond to a nucleation growth process of the same type ($n = 2$) for the two transformations $C_1 \rightarrow C_2 \rightarrow C_2$. If we assume a thermal process the growth is monodimensional.

1. Introduction

For several years, the polymorphism of frozen liquid crystals obtained by fast cooling the nematic phase has been investigated (for example 4-methoxybenzylidene-4′-*n*-butylaniline (MBBA) and OH-MBBA). Fast cooling down to 100 K provides a vitreous state which we can consider as a frozen state of the nematic phase. On reheating this glass turns into different solid states which are steps between the glassy to the crystalline materials.

In the case of 4-ethoxybenzylidene-4′-*n*-butylaniline (EBBA) Kirov *et al.* [1] asserted that by fast cooling, they obtained at low temperature a glassy liquid crystal. The other authors who also made such a study, never found this result whatever the quench rate used. In particular, Sorai *et al.* [2] observed by DTA, with a quench rate of 500 K min^{-1} an exothermic peak at about 20°C which corresponds to the transition from a nematic state to a metastable crystalline state. In the same way, Yasuniwa *et al.* [3], have shown with a quench rate of 12·8 K min^{-1} by DSC that an exothermic peak appeared between 3°C and 7°C also giving a metastable phase. Our own experiments confirm that whatever the quench rate we have used, we never obtained a vitreous phase. Many experiments have already been performed on the phase transitions and the polymorphism of the frozen liquid crystal EBBA. Differential scanning calorimetry, X-ray and neutron diffraction, as well as Raman scattering [4] have been used to determine structural and dynamical properties of the different solid states under different conditions of cooling and reheating.

We have returned to X-ray diffraction for essentially two reasons:

(1) the different phases which appear have not been clearly characterized; the experimental set up we have used allows us to record diffraction spectra exactly and to determine local order and long range order in the different phases.

---

* Author for correspondence.

0267–8292/91 $3·00

(2) it is necessary for an unambiguous determination of the different phases to quench the material rapidly and then to reheat the sample slowly. According to the temperature, the transformation rate of the metastable phase is either negligible or sufficient to observe the transformation. We have been able to locate the metastability zone for the material and to study inside the corresponding temperature range, at a given temperature the rate of the transformation from one metastable phase to another one, i.e. we have performed a kinetic study of the phase transformations.

2. Experimental set up

We have used a multidetector in order to collect a large amount of data easily. The nematogen EBBA was purified by successive recrystallizations from ethyl alcohol from the commercial product provided by Aldrich at 98 per cent. The sample, solid at room temperature, is introduced in a Lindeman glass capillary 1 mm in diameter and 10 mm long and then melted to the isotropic liquid ($T_{NI} = 353$ K). This capillary tube is set in a goniometer head, the movements of which allow the tube to be brought into coincidence with the incident beam and to adjust it along a vertical axis. It can be rotated continuously (1 rpm) around the vertical axis in order to average over all orientations perpendicular to the rotation axis. The X-ray beam (Cu Kα, 40 kV, 20 mA, $\lambda = 1{\cdot}5418$ Å) is monochromatized by the (002) Bragg reflection of a plane pyrolitic graphite monochromator; its divergence is reduced by a $\phi = 0{\cdot}8$ mm cylindrical collimator. The multidetector is a gas flow type with a curved anode (INEL CPS 120); the sample is set at its centre. The X-photons scattered in the equatorial plane are measured over 120°, with a resolution of 0·03°, the window height being 8 mm. In order to check the sample adjustment the detector was arranged symmetrically with respect to the incoming X-ray beam which was stopped in front of the counter by a hollow lead beam stop. This allowed us to measure as close as 3·5° to the incident beam. The electronic system of the diffractometer includes control for gas flux and pressure, the high voltage, the discrimination of the pulses coming from the detector, allow us to determine through delay lines the position of the detected photons and their intensity. A 4 k multichannel analyser provides a preliminary storage. The spectra were stored in a personal computer for further data treatment. The instrumental width is about 10 channels (0·30°) FWHM and the incoming beam shape is gaussian. The temperature was controlled to about 0·5 K precision with a nitrogen gas flow cryostat (modified ENRAF-NONIUS cryostat). It allows quenching faster than 40 K mm^{-1}. To perform this, it is sufficient to move, abruptly, the flow on the top of the sample.

3. Polymorphism of EBBA

The melting point T_{CN} for the stable crystal is 309 K [5] and the transition temperature from the nematic to the isotropic phase is 352·6 K. From the nematic phase two ways can be used to provide different structural modifications.

On slow cooling, from the isotropic phase, the nematic phase is supercooled and, at about 286 K, turns into a phase, the X-ray diagram of which looks like that of the phase which we later denoted C_2 (see figure 1). This phase is not identical to the stable phase C_4 obtained by recrystallization in petroleum ether, the structure of which has been determined by Howard *et al.* [6].

On fast cooling the nematic phase, we always obtain a phase, denoted C_1, different from a frozen nematic phase whatever the quench rate. From this quenched state the sample was then annealed by a slow increase of the temperature (in the range of some

K min^{-1}) until the phase transition began. The temperature was then kept constant until the transformation was complete. The kinetics study which will be reported in the fourth part of this paper allows us to see when the transformation can be considered as complete and to avoid a study of a mixture of several phases because of a partial transformation. We can, at the end of the transformation, decrease the temperature to stabilize the phase in a domain where the transformation rate is negligible. However, the X-ray spectra, which we show in figures 1 and 2, have been performed at the transformation temperature. A qualitative analysis of the shape and the position of the peaks has been made, by fitting them to gaussian or lorentzian functions.

3.1. *Discussion of the results*

(1) Nematic phase. The nematic phase (see figure 1) obtained at room temperature on cooling the isotropic phase is characterized by a wide diffuse peak at $Q = 1{\cdot}5\,\text{Å}^{-1}$ called the liquid ring. The peak can be decomposed into two lorentzians, the width at half maximum of which is $\Delta Q_1 = 0{\cdot}43\,\text{Å}^{-1}$ and $\Delta Q_2 = 0{\cdot}50\,\text{Å}^{-1}$ and corresponds to an average correlation length L_r of 21 Å deduced from the Hosemann formula $\Delta Q = 10/L_r$ [7, 8].

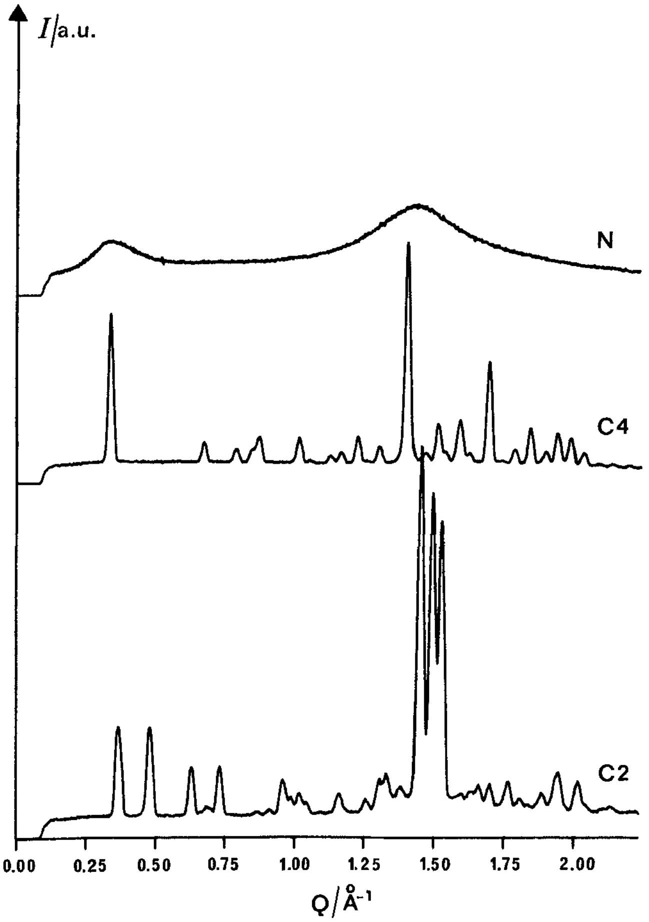

Figure 1. X-ray diffraction spectra of the nematic phase N, the crystalline phase C_4 and the C_2 phase obtained on slow cooling from the nematic phase of EBBA.

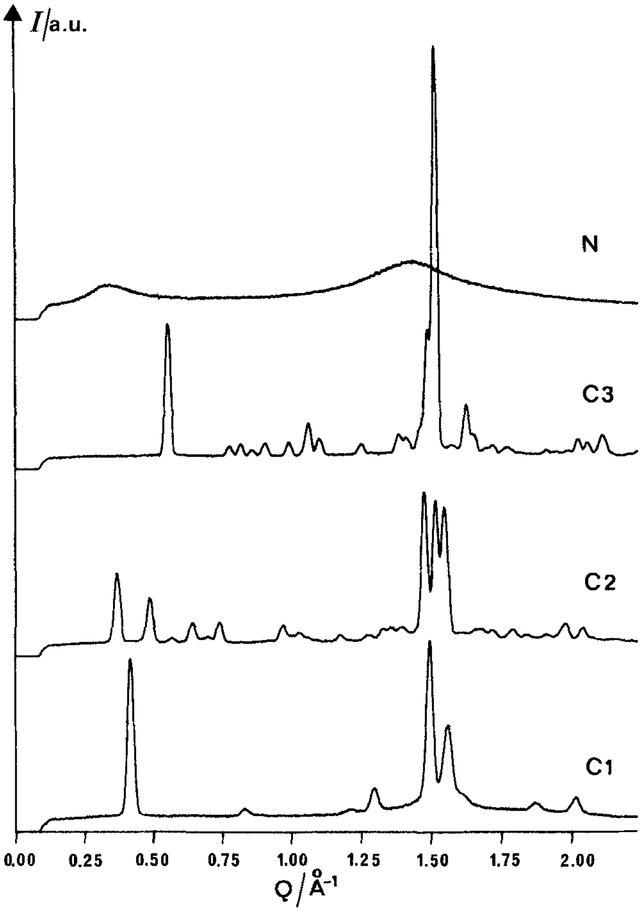

Figure 2. X-ray diffraction spectra of the nematic phase N, the quenched phase C_1 and the phase C_2 and C_3 obtained on reheating of the C_1 phase of EBBA.

Table 1. Characteristics of the diffraction lines in the C_1 phase. G_n, L_n denote respectively gaussian or lorentzian lines; Q and ΔQ are the position and width at half maximum, respectively.

Type	I/u.a.	Q/Å^{-1}	ΔQ/Å^{-1}
G_1	39651·28	0·4133	0·0229
G_2	1925·94	0·8287	0·0302
G_3	736·22	1·2134	0·0336
G_4	4592·69	1·2951	0·0274
G_5	46029·63	1·4972	0·0229
G_6	17950·93	1·5605	0·0229
G_7	1649·19	1·6121	0·0212
G_8	2279·33	1·8702	0·0716
G_9	5286·64	2·0173	0·0369
L_1	4639·63	1·5658	0·3651

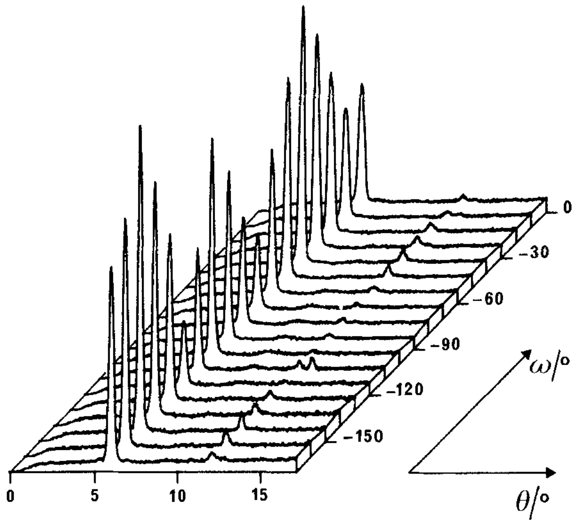

Figure 3. X-ray diffraction spectra of EBBA aligned in its nematic phase by a magnetic field of 0·8 T. The initial position $\omega = 0$ corresponds to the magnetic field perpendicular to the incoming beam, ω is the rotation of the sample, 2θ the diffraction angle.

(2) Phase C_1 (see figure 2). If we compare this to the nematic phase, we see the appearance of a sharp, intense peak at a low value of $Q = 0{\cdot}413\ \text{Å}^{-1}$ and several peaks appear at the liquid ring position. Table 1 shows that the sharp peaks are gaussian, the width of which corresponds approximately to the apparatus resolution. In addition, the spectrum exhibits an important continuous background which can be represented by a lorentzian with a correlation length of 27 Å. From table 1, we see that second and third order of the peak Q at $0{\cdot}413\ \text{Å}^{-1}$ also exists. Our interpretation of this feature is that, because of the molecular mobility due to the thermal energy, a layered reorganization occurs characterized by a long range order of smectic layers. The thickness of these layers, 15 Å, compared with the molecular length, 20 Å, reveals that the molecules are inclined at an average angle of 40° to the normal of the smectic planes. To confirm this, we have also attempted to align the director of the nematic phase with a magnetic field of 0·8 T and then quenched the system. Figure 3 shows that, although we have not obtained a monodomain, we observe the maximum for the smectic line by a rotation of the sample by $35° \pm 5°$ with respect to the initial field direction.

At the liquid ring position, sharp gaussian peaks appear (see table 1) and lead us to think that the molecules are locally arranged in each layer in a lattice. However, the determination of the interreticular distances are, with our equipment, too imprecise to obtain for certain the elementary cell, the spatial group, and to index in an unequivocal way the spectral lines. All of the experiments we have performed seem to show that we have a three dimensional order and so this phase may be described as a crystal smectic. Moreover, under the preceding peaks, the lorentzian line with a maximum at Q of $1{\cdot}57\ \text{Å}^{-1}$ shows us that it subsists in this phase an important disorder.

(3) Phase C_2. On reheating between 217 K and 225 K, the phase C_1 turns into a phase C_2. Its X-ray pattern is shown in figure 2. This transformation corresponds to important changes. The smectic peak of the C_1 phase completely disappears in the C_2 phase. Many sharp lines appear distributed on the accessible angular interval. The

Table 2. Characteristics of the diffraction lines in the C_2 phase.

Type	I/u.a.	$Q/Å^{-1}$	$\Delta Q/Å^{-1}$
G_1	13333·56	0·3661	0·0243
G_2	9622·28	0·4830	0·0237
G_3	1259·25	0·5666	0·0177
G_4	3815·75	0·6362	0·0242
G_5	958·79	0·6951	0·0329
G_6	3976·61	0·7368	0·0242
G_7	3029·24	0·9675	0·0325
G_8	1497·05	1·0283	0·0704
G_9	1137·44	1·1698	0·0216
G_{10}	910·95	1·2782	0·0251
G_{11}	2080·01	1·3258	0·0286
G_{12}	2023·01	1·3566	0·0163
G_{13}	1759·18	1·3936	0·0485
G_{14}	34184·29	1·4761	0·0234
G_{15}	33162·36	1·5173	0·0236
G_{16}	27231·62	1·5499	0·0235
G_{17}	1529·24	1·6753	0·0534
G_{18}	1470·03	1·7225	0·0304
G_{19}	2163·90	1·7959	0·0376
G_{20}	1208·15	1·8420	0·0380
G_{21}	1208·15	1·9131	0·0769
G_{22}	3872·87	1·9756	0·0330
G_{23}	2547·02	2·0412	0·0511
G_{24}	969·75	2·1606	0·1302
G_{25}	355·89	2·2536	0·0413
L_1	3049·69	1·5652	0·3951

analysis of these lines, given in table 2, shows that their widths are equal to the apparatus resolution; the slightly larger widths of some lines are probably due to the superimposition of several lines. The corresponding order is necessarily three dimensional. We can consider that the C_2 phase is then constituted by crystalline domains, the dimensions of which are comparable to the correlation length. An approximate value of this correlation length L_r is given by the Hosemann formula with a ΔQ value which is given by the resolution $L_r = 10/\Delta Q$ of 500 Å. In this phase, disorder still exists, it is represented by the L_1 lorentzian, its maximum has practically the same position as that of the lorentzian in C_1 but with a weaker intensity.

(4) Phase C_3. Between 230 K and 245 K, the phase C_2 turns into the phase C_3. Its X-ray pattern is shown in figure 2 and the analysis of its peaks in table 3. Most of the X-ray lines have a width approximately equal to the resolution. The wider lines can be interpreted as due to the superimposition of several lines. The continuous background presented in C_2 now has totally disappeared. This phase is stable up to room temperature and turns into the nematic phase at 307 K. Contrary to the opinion of Dolganov [4], we have never observed the transition from the C_3 phase to the C_4 phase.

In conclusion, quenched EBBA shows on slow reheating metastable phases which are more and more ordered. The C_1 phase is a monolayer smectic phase; the molecules are inclined at an angle of $35° \pm 5°$ to the normal of the smectic planes. If we compare the MBBA phases studied by Pépy *et al.* [9] we see that the polymorphism of EBBA is less rich than that of MBBA. In MBBA, we observe a vitreous phase C_0, two bilayer smectic phases C_1 and C_2 and two crystalline phases C_3 and C_4.

Table 3. Characteristics of the diffraction lines in the C_3 phase.

Type	I/u.a.	$Q/\text{Å}^{-1}$	$\Delta Q/\text{Å}^{-1}$
G_1	196644·52	0·5495	0·0217
G_2	13893·38	0·7743	0·0214
G_3	17642·75	0·8149	0·0231
G_4	9975·04	0·8566	0·0217
G_5	19661·23	0·9035	0·0312
G_6	23906·83	0·9910	0·0235
G_7	51242·19	1·0613	0·0259
G_8	26874·36	1·0996	0·0229
G_9	16818·27	1·2495	0·0478
G_{10}	17068·98	1·3841	0·0123
G_{11}	32245·93	1·4116	0·0666
G_{12}	45125·86	1·4603	0·0225
G_{13}	226011·00	1·4887	0·0236
G_{14}	760954·56	1·5162	0·0189
G_{15}	20485·61	1·5774	0·0967
G_{16}	90940·40	1·6216	0·0193
G_{17}	34722·22	1·6521	0·0222
G_{18}	11271·64	1·7246	0·0459
G_{19}	12589·42	1·7729	0·1246
G_{20}	10624·92	1·9120	0·1368
G_{21}	26642·20	2·0235	0·0254
G_{22}	23591·70	2·0547	0·0238
G_{23}	30220·75	2·1128	0·0440
G_{24}	8937·56	2·2474	0·0498

4. Kinetics of the phase transformations

We have been lead to study the kinetics of the successive phase transformations in EBBA at different temperatures. Indeed if we want to characterize a phase correctly, we have to be sure that the corresponding system does not involve a mixture of phases. When we reheat the frozen EBBA at a constant rate, we are not sure that a transformation from the C_n phase to the C_{n+1} phase is achieved before the transformation from C_{n+1} to C_{n+2} begins. On the other hand, detailed study of the kinetics will also provide information on the mechanism of the transformation.

4.1. *Experimental determination of the kinetics*

For the experimental study of the transformations C_1 to C_2 and C_2 to C_3, we have chosen to look at the evolution of well-isolated X-ray diffraction lines. That is to say:

(1) The disappearance of the smectic peak of the C_1 phase at $Q = 0{\cdot}413\,\text{Å}^{-1}$ to study the transformation C_1 to C_2.

(2) The appearance of the X-ray line at $Q = 0{\cdot}57\,\text{Å}^{-1}$ which allows us to follow the transformation C_2 to C_3. In this later observation, we neglect the intensity of the line of the C_2 phase at $Q = 0{\cdot}58\,\text{Å}^{-1}$. Its intensity is less than one per cent of that at $Q = 0{\cdot}57\,\text{Å}^{-1}$. It would also be possible to use the disappearance of the C_2 lines at $Q = 0{\cdot}37\,\text{Å}^{-1}$ and $Q = 0{\cdot}50\,\text{Å}^{-1}$. We have verified that we obtained with the intensity of the later lines the same results as from the intensity of the line considered.

Figure 4 shows us the observed spectra during the two transformations.

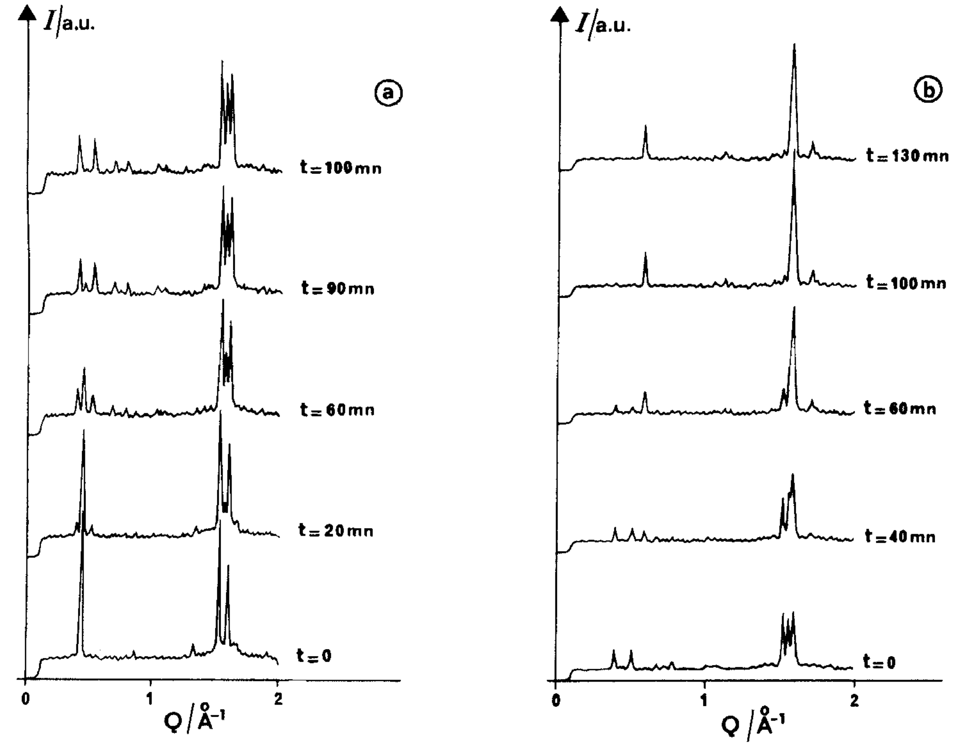

Figure 4. Kinetics of transformations of EBBA (*a*) $C_1 \rightarrow C_2$, (*b*) $C_2 \rightarrow C_3$ X-ray spectra measured as a function of time.

Kinetics have been measured at constant temperature at three temperatures 221 K, 223 K and 225 K for the transformation $C_1 \rightarrow C_2$ and at 235 K and 238 K for the $C_2 \rightarrow C_3$ transformation under the same experimental conditions. The integrated intensity, being proportional to the irradiated volume of the phase considered, the fractional volume $X'(t)$ of C_1 and $X(t)$ of C_2 in the mixture (C_1, C_2) is given by

$$X'(t)=1-X(t)=\frac{I(t)-I(\infty)}{I(0)-I(\infty)}.$$

It is also the fractional volume of C_2 and C_3 in the mixture (C_2, C_3).

After quenching the nematic phase which gives the C_1 phase, we reach the temperature of the chosen transformation by fast reheating so that, during this increase of the temperature, the C_1 phase undergoes no transformation. When the requisite temperature is attained, we keep it constant and we record the X-ray spectra at regular periods. As the kinetics are relatively fast, we limit the time of each period to 5 min which introduces non-negligible statistical errors. When the transformation of the system to C_2 is complete, we rapidly increase the temperature in order to reach the transformation temperature chosen to study the transformation of the system in C_3. The recordings were also performed every 5 min.

Since the width of studied lines are constant, we use the intensity of the line maximum as the integrated intensity. The curves $X'(t)$ or $X(t)$ obtained have a sigmoidal shape and can be fitted by a function which represents the Avrami law. For each experiment, we determine the time at which the transformation has gone to half completion, i.e. $X(t_{1/2})=0{\cdot}5$ and by using $t_{1/2}$ as the time unit, we see that for a given transformation, the curve $X'(\tau)$ or $X(\tau)$ with $\tau=t/t_{1/2}$ is a universal curve independent of temperature (see figure 5 for $C_1 \rightarrow C_2$ and figure 6 for $C_2 \rightarrow C_3$). For the transformation $C_1 \rightarrow C_2$ the times of half completion $t_{1/2}$ are an increasing function of temperature as shown in table 4. In the case of the transformation $C_2 \rightarrow C_3$, the times of half completion are approximately the same.

Table 4. Time of half completion $t_{1/2}$ versus the temperature.

T/K	$t_{1/2}$/min
221	24
223	30
225	40

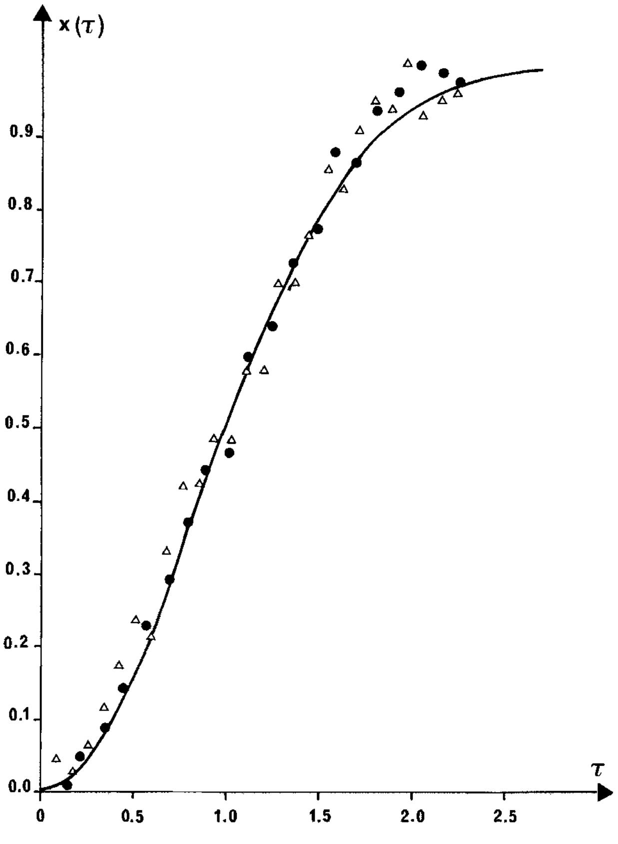

Figure 5. Fractional volume of the C_1 phase in the mixture (C_1, C_2) versus the reduced time $\tau=t/t_{1/2}$ where $t_{1/2}$ is the time of half completion (—, $\exp(-\tau^2)$; ○, $T=221$ K; △, $T=223$ K; ●, $T=225$ K).

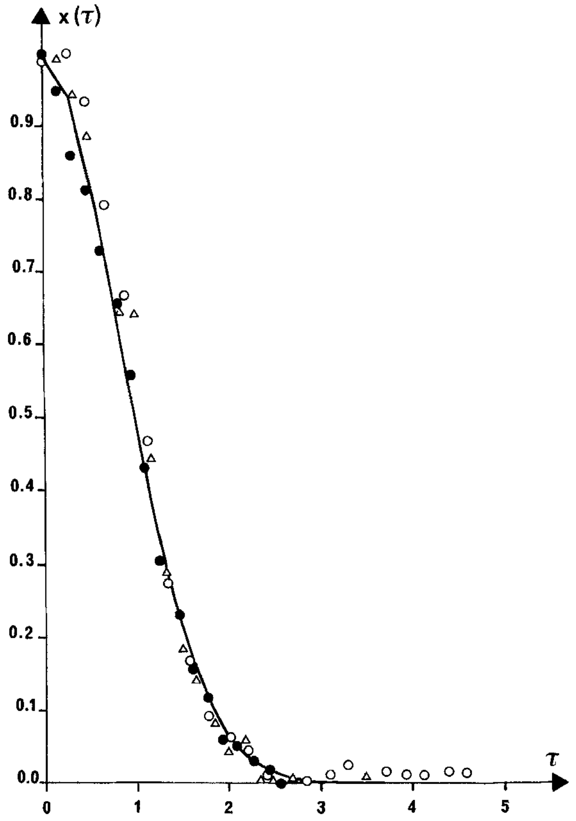

Figure 6. Fractional volume of the C_3 phase in the mixture (C_2, C_3) versus the reduced time τ (—, $1-\exp(-\tau^2)$; △, $T=238$ K; ●, $T=235$ K).

4.2. *Interpretation*

There is a close analogy between the classical first order transition and the transitions between the metastable states obtained from a frozen liquid crystal. Any metastable state is stable against small amplitude fluctuations but unstable against large amplitude fluctuations. In the classical theory of first order transitions, thermal fluctuations with large amplitude create nuclei of the more stable phase. These nuclei grow if their size goes beyond a critical size. The kinetics depend, therefore, on the nucleation rate, J, i.e. the number of nuclei which have the critical size per unit volume and unit time. In general the nucleation rate can be expressed by

$$J=J_0\exp\left(-\frac{\Delta G^*}{kT}\right),$$

where ΔG^* is an activation energy for nucleation. For a first order transition, according to the classical theory ΔG^* depends on the supercooling $\Delta T=T_c-T$ where T_c is the equilibrium transition temperature and $\Delta G^*=K/(\Delta T)^2$. When the kinetic is nucleation limited, the phase transformation period is inversely proportional to the nucleation rate and, so, is a decreasing function of ΔT. For metastable phases of a frozen liquid crystal, the situation is more complicated since to go from a metastable phase to the stable phase, we have to go through several intermediate steps and that, for these intermediate steps, it is not possible to define a transition temperature.

After nucleation, having their critical size, nuclei grow with a constant domain-walk velocity, the value of which in an anisotropic medium depends on the direction inside the nuclei. If, for example, in a grain, molecules are arranged in smectic layers, we may have the following two extreme cases:

(1) the velocity of growth V_N in the perpendicular direction to the planes of the layers is large with respect to the velocity of growth V_T parallel to the planes of the layers, the growth is then unidimensional and d the dimensionality of the nuclei is equal to 1,

(2) if, in contrast, $V_T \gg V_N$, the growth of the nuclei is two dimensional and d is equal to 2.

An explicit expression for the transformed fractional volume $X(t)$ for this model was first given by Kolmogorov [11], then later independently by Avrami [12] and explicitly by Johnson and Mehl [13] (see also [10])

$$X(t)=1-\exp\left[-\frac{D}{d+1}Jv^d t^{d+1}\right],$$

$$D=2,\pi,\frac{4\pi}{3}\quad \text{for}\quad d=1,2,3,$$

if $d=1$, $v=V_N$ and if $d=2$, $v=V_T$. From this explicit Avrami law, we see that a single characteristic scale time exists $t_0=((D/d+1)Jv^d)^{-1/d+1}$ and this law can be expressed in terms of the scale time $\tau=t/t_0$ and becomes a universal law

$$X(\tau)=1-\exp(-\tau^{d+1}),$$

t_0 is related to the time of half completion by

$$t_{1/2}=t_0(\log_e 2)^{1/d+1}.$$

If we assume that during the quenching, nuclei of the C_2 phase are in addition created, with the same matrix, we would have an athermal growth of the C_2 phase. Under these conditions, the phase transformation would be determined only by the growth velocity and then we would obtain

$$X(t)=1-\exp(-NDv^d t^d),$$

where N is the number of grains per unit volume. With the characteristic scale time $t_0=(DNv^d)^{-1/d}$ and $\tau=t/t_0$ the transformed fractional volume becomes

$$X(\tau)=1-\exp(-\tau^d).$$

We have, therefore, fitted the experimental curves to the law

$$X(t)=1-\exp(-At^n).$$

Whether this fit is for the transformation from $C_1 \rightarrow C_2$ at different temperatures, or for the transformation from $C_2 \rightarrow C_3$ we find $n=2$. So, if the nucleation was thermal, $d=1$ and the growth would be one dimensional. Nuclei then appear in the shape of needles. If, on the contrary, the nucleation was athermal, the growth would be two dimensional and the nuclei would be the shape of plaquettes.

The dimensionality of the grains could be obtained by a direct observation with an optical microscope. Some photographs presented in the paper of Yasuniwa [14] seem to indicate that the grains have a needle shape, i.e. $d=1$. Moreover, if we can admit that during the quench, nuclei of the C_2 phase would be formed, it is more difficult to assume that it also appears by quenching nuclei of the C_3 phase. It is, therefore, more reasonable to assume thermal nucleation and hence $d=n-1=1$.

5. Conclusion

We have characterized the different metastable phases obtained by reheating the frozen liquid crystal EBBA by measuring the interreticular distances and by the determination of the shape of the X-ray lines. The C_1 phase is a crystal smectic phase, the others are crystalline. The sequence of the metastable phases, which we have obtained, only differs by the existence of the C_1 phase from the sequence of the stable phases obtained on slow cooling. On slow cooling we obtain from the nematic phase an identical phase to the C_2 phase. This later phase can eventually evolve to a C_3 or C_4 phase.

The kinetics for the transformation of the metastable phases correspond to a nucleation growth process of the same type ($n=2$) for the two transformations $C_1 \rightarrow C_2 \rightarrow C_3$. Additional observations, in particular, with an optical microscope will be necessary to determine more exactly the dimensionality of the grains. Many accurate measurements for the incubation time and the time of half completion versus temperature would allow a better approach of the mechanism of these transformations.

References

[1] Kirov, N., Fontana, M. P., and Cavatorta, F., 1979, *Molec. Crystals liq. Crystals*, **54**, 207; Kirov, N., and Fontana, M. P., 1980, *Molec. Crystals liq. Crystals Lett.*, **56**, 195; Cavatorta, F., Fontana, M. P., and Kirov, N., 1977, *Molec. Crystals liq. Crystals Lett.*, **34**, 241.

[2] Sorai, M., Nakamura, T., and Seki, S., 1974, *Bull. chem. Soc. Japan*, **47**, 2192.

[3] Yasuniwa, M., and Minato, K., 1982, *Molec. Crystals liq. Crystals*, **87**, 97.

[4] Dolganov, V. K., Gal, M., Kroo, N., Rosta, L., and Szabon, J., 1987, *Liq. Crystals*, **2**, 73.

[5] Dolganov, V. K., Kroo, N., Rosta, L., Sheka, E. F., and Szabon, J., 1985, *Molec. Crystals liq. Crystals*, **127**, 187.

[6] Howard, J., Leadbetter, A. J., and Sherwood, J. W., 1980, *Molec. Crystals liq. Crystals*, **56**, 271.

[7] Vainshtein, B. K., 1966, *Diffraction of X-rays by Molecular Chains* (Elsevier).

[8] Guinier, A., *Théorie et Technique de la Radiocristallographie* (Dunod).

[9] Pépy, G., Fouret, R., More, M., and Rosta, L., 1989, *Physica Scripta*, **39**, 485.

[10] Hamaya, N., Yamada, Y., Axe, J. D., Belanger, D. P., and Shapiro, S. M., 1986, *Phys. Rev.*, **33**, 7770.

[11] Kolmogorov, A. N., 1937, *Bull. Acad. Sci. U.S.S.R. Phys. Ser.*, **3**, 555.

[12] Avrami, M., 1939, *J. chem. Phys.*, **7**, 1103; 1940, *Ibid.*, **8**, 212; 1941, *Ibid.*, **9**, 177.

[13] Johnson, W. A., and Mehl, R. F., 1939, *Trans. Am. Inst. Min. Metall. Pet. Eng.*, **135**, 416.

[14] Yasuniwa, M., 1988, *Molec. Crystals liq. Crystals* B, **158**, 279.